


<b>REPORT DOCUMENTATION PAGE</b> <b>AD-A279 344</b> 			Form Approved OMB No. 0704-0188
<small>ated to average 1 hour per response, including the time for reviewing instructions, searching existing data sources, reviewing the collection of information. Send comments regarding this burden estimate or any other aspect of this burden, to Washington Headquarters Services, Directorate for Information Operations and Reports, 1215 Jefferson Office of Management and Budget, Paperwork Reduction Project (0704-0188), Washington, DC 20503.</small>			
1. DTI DATE		3. REPORT TYPE AND DATES COVERED <b>FINAL</b>	
4. TITLE AND SUBTITLE <b>A New Concept of a Low-Frequency Underwater Sound Source</b>		5. FUNDING NUMBERS PE - OMNR WU - DN152-144	
6. AUTHOR(S) D. M. Donskoy and J. E. Blue			
7. PERFORMING ORGANIZATION NAME(S) AND ADDRESS(ES) NAVAL RESEARCH LABORATORY Underwater Sound Reference Detachment P.O. Box 568337 Orlando, FL 32837		8. PERFORMING ORGANIZATION REPORT NUMBER	
9. SPONSORING / MONITORING AGENCY NAME(S) AND ADDRESS(ES) COMMANDER NAVAL SEA SYSTEMS COMMAND WASHINGTON, DC 20362-5101		10. SPONSORING / MONITORING AGENCY REPORT NUMBER	
11. SUPPLEMENTARY NOTES Published in J. Acoust. Soc. Am. 95(4), April 1994, pp. 1977-1982.			
12a. DISTRIBUTION / AVAILABILITY STATEMENT Approved for public release; distribution unlimited.		12b. DISTRIBUTION CODE	
13. ABSTRACT (Maximum 200 words) A new concept of a low-frequency (< 1000-Hz) underwater sound source has been developed and tested. The oscillation of a rigid body and a means for converting the dipole oscillation of the body to monopole radiation are used in this source. The source can be powered with electric or linear motors or hydrodynamic exciters that convert tow or flow to vibration. To prove the concept, a small version of the electric motor powered source has been built and successfully tested. To extend the bandwidth of the source, the variable resonance frequency and multiresonances of the device are discussed. A gas spring with a frequency-dependent stiffness is employed for the multifrequency resonant source design. The source promises to be reliable, inexpensive, highly efficient, and powerful.			
14. SUBJECT TERMS Transducers                      Sonar                                      Projector Sound Source                      Low Frequency Source                      Sound Projector Underwater Acoustics			15. NUMBER OF PAGES 6
			16. PRICE CODE
17. SECURITY CLASSIFICATION OF REPORT <b>UNCLASSIFIED</b>	18. SECURITY CLASSIFICATION OF THIS PAGE <b>UNCLASSIFIED</b>	19. SECURITY CLASSIFICATION OF ABSTRACT <b>UNCLASSIFIED</b>	20. LIMITATION OF ABSTRACT <b>UL</b>

**DTIC**  
**ELECTE**  
**MAY 18 1994**

94 5 17 019

# A new concept of a low-frequency underwater sound source

Dimitri M. Donskoy

Davidson Laboratory, Stevens Institute of Technology, Castle Point on the Hudson, Hoboken, New Jersey 07030

Joseph E. Blue

Naval Research Laboratory, Underwater Sound Reference Detachment, Orlando, Florida 32856-8337

(Received 31 August 1993; accepted for publication 15 December 1993)

A new concept of a low-frequency ( $< 1000$ -Hz) underwater sound source has been developed and tested. The oscillation of a rigid body and a means for converting the dipole oscillation of the body to monopole radiation are used in this source. The source can be powered with electric or linear motors or hydrodynamic exciters that convert tow or flow to vibration. To prove the concept, a small version of the electric motor powered source has been built and successfully tested. To extend the bandwidth of the source, the variable resonance frequency and multiresonances of the device are discussed. A gas spring with a frequency-dependent stiffness is employed for the multifrequency resonant source design. The source promises to be reliable, inexpensive, highly efficient, and powerful.

PACS numbers: 43.38.Ar, 43.30.Yj

94-14751  


NRL/USRD  
416 470

## INTRODUCTION

The advent of new ocean research fields such as acoustic tomography, the expansion of existing fields such as marine geology and mineral resource exploration, the development of new applications such as acoustic thermometry of the ocean (ATOC and GAMOT projects), and installation of ultradistant early warning submarine detection sonar systems,<sup>1-4</sup> require powerful and reliable low-frequency underwater sound radiators that operate in the frequency range of tens to hundreds of hertz.

In order to be effective, such radiators must function reliably for years without maintenance; provide a high source level, be highly efficient, provide broadband frequency performance, and be submersible to significant ocean depths (on the order of 1000 m). Combining all of these requirements in one radiator in the frequency range below 1000 Hz presents a set of very difficult and conflicting tasks.

It is well known that high efficiency and high acoustic power output for a small (compared to the wavelength) radiator can be achieved using a resonant monopole-type transducer at a large volume velocity. This fact requires large displacements and creates large material deformations for conventional designs, which can lead to fatigue failures. Also, the requirement for a resonant transducer design from a projector that is small compared to a wavelength contradicts the broadband requirement. Other major drawbacks are excess friction from seals between the radiating piston and the housing of the radiator and the high cost of the conventional low-frequency sound sources. As frequency is lowered, it becomes even more difficult to satisfy these contradictory requirements using conventional transducer types. Accordingly, the development of novel transducers satisfying these conflicting requirements at low frequencies is extremely challenging.

## I. DESCRIPTION OF THE SOURCE

### A. Dipole-to-monopole convertor

Below we describe a new approach for developing low-frequency (LF) radiators.<sup>5</sup> As mentioned, the main causes of low reliability of LF radiators are the large deformations of the radiating surface or its suspension, which leads to fatigue failures of the materials. However, in order to generate a high source level of sound at low frequencies it is necessary to create large displacements of the radiating surface. To satisfy the two conflicting requirements (large displacement of the radiating surface and small deformation of materials) we propose using the oscillation of a rigid body to provide large displacement without deformation and an arrangement for converting a dipole oscillation of the rigid body to a monopole radiation.

A diagram of the radiator is shown in Fig. 1. Here, 1 is the oscillating rigid body having positive buoyancy, 2 is the chamber, and 3 is the spring. It can be a typical spring [Fig. 1(a)] or just an air volume inside the chamber [Fig. 1(b)], which has its own stiffness. The chamber with the floating body is held in a vertical position in order to retain air inside the cylinder. The vertical orientation of the chamber is maintained by establishing a center of gravity for the assembly lower than its geometric center. Such orientation allows the retention of air or another gas inside the chamber without special seals, diaphragm, etc. The gap between the chamber and the floating body has to be small in order to minimize fluid flow in the gap at working frequencies of the radiator.

Figure 2 shows the equivalent mechanical and electrical diagrams, where  $M_1$  is the mass of the floating body plus its added mass of water,  $M_2$  is the mass of the chamber plus its added mass of water,  $F$  is the vibromotive force,  $k$  is the stiffness of the spring (or the air volume),  $R_m$  is the mechanical resistance (it describes mechanical dissipation of energy in the system), and  $R_{a1}$  and  $R_{a2}$  are

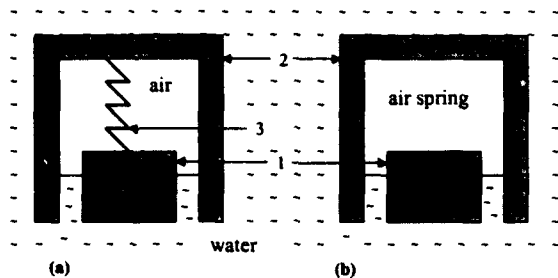


FIG. 1. A diagram of the radiator: (a) mechanical spring version, (b) air spring version.

the radiation resistances for the piston surface of the float and the chamber.

A generator of vibromotive force  $F$  is placed inside the float and the force (or its component) is applied in the vertical direction. The vibromotive force causes vertical oscillations (vibrations) of the rigid body and (through the spring or the air volume) the chamber. If the resistance of the system is small compared to its reactance, this system resonates with frequency

$$\omega_r \approx \sqrt{\omega_1^2 + \omega_2^2} \quad (1)$$

where  $\omega_{1,2}^2 = k/M_{1,2}$  and  $\omega$  is the force frequency. It is easy to show that at resonance the oscillation velocities  $u_1$  and  $u_2$  of the chamber and the body have opposite signs; i.e.,  $u_2 \approx -(M_1/M_2)u_1$ . Therefore, in the vicinity of resonance, we have a device for the conversion of dipole oscillation of the rigid body to monopole pulsation of the body-spring-chamber system. The radiating surfaces (piston surfaces of the chamber and the body) undergo no deformations.

There can be another mode of operation if  $M_2 \gg M_1$ . This can be done by increasing the added mass of water coupled to the chamber simply by attaching a larger-diameter plate on top of the chamber. In this case the chamber will remain substantially stationary while the float moves and radiates sound as a one-sided monopole radiator.

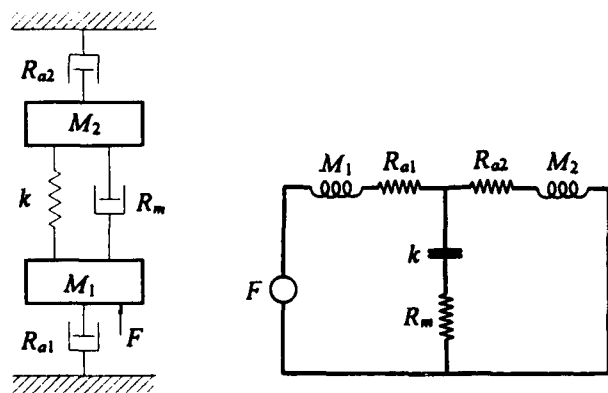


FIG. 2. The equivalent mechanical and electrical diagrams.



FIG. 3. Picture of the experimental source and its components.

## B. Generation of vibromotive force

Various methods can be employed to generate the vibromotive force, such as oscillation of a massive body (shaker) within the floating body. Because the center of mass of the float must remain fixed, the oscillation of the shaker causes the oscillation of the float. For high reliability and high efficiency it is better (and less expensive) to use commercially available components. For example, an electric motor with an unbalanced mass that is commonly used for various industrial applications (such as a bin vibrator, feeders, screeners, vibro-testing vibrators) meets the reliability requirement. This unit operates in an appropriate frequency range, it has very high efficiency (more than 90%), and can operate without maintenance for well over 10 years [for example, a \$2000 commercially available vibrator weighing 90 kg can generate 22 250 N (5000 lb) of force].

It is also possible to use a linear electric motor, which is more suitable for generating a phase-modulated signal. High force brushless linear motors have no physical contact between motor parts; hence, no maintenance is needed.

The vibromotive generator can alternatively utilize a device for converting hydrodynamic excitation from water flow around the radiator, which may occur during towing or other external translational movement of the pulsator assembly, into vibromotive force. Such a device is described in Ref. 6.

## C. Test

In order to prove the concept of the radiator and to get initial information for designing a full scale prototype of the source, we have built a small-scale prototype. This source was built and tested in August–September, 1992, at Davidson Laboratory, Stevens Institute of Technology. The test was performed in the laboratory's 75-ft<sup>2</sup> tank.

The source has two cylindrical parts and a spring, as shown in Figs. 1(a) and 3, with external diameter of 0.32 m (12.75 in.). The vibromotive generator (ordinary electric motor with eccentric masses) is placed into the internal cylinder. The motor and, therefore, the radiator, runs in a frequency range from a few hertz up to 150 Hz. The

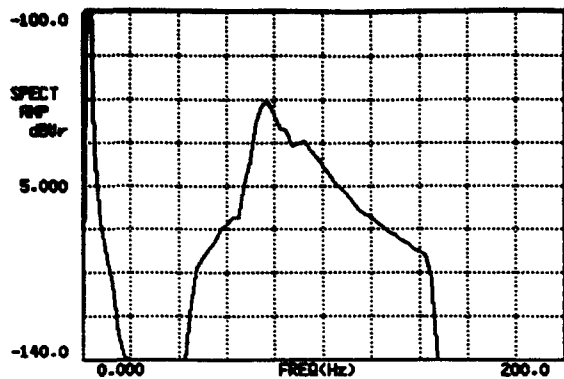


FIG. 4. Measured frequency response of the experimental source.

resonance frequency of the radiator depends on the stiffness of the spring. During the test the resonance frequencies (for different springs) were 35, 63, and 77 Hz. Accelerometers were installed on the top and bottom of the source to measure vibrations of the radiating surfaces. Based on these measurements we were able to determine the phase difference of vibrations of the radiating surfaces, radiated power,  $Q$  factor, and mechanical (viscous) resistance of the radiator.

The measurements show that the source operates as a monopole, according to the concept. The radiated power is 24 W at frequency 77 Hz. The measured frequency response of the experimental source is shown in Fig. 4.

## II. SOURCE LEVEL, BANDWIDTH, AND EFFICIENCY

For an omnidirectional source, the source level (SL) is defined by the equation<sup>7</sup>

$$SL = 10 \log W + 170.8 \text{ dB re: } 1 \mu\text{Pa at } 1 \text{ m}, \quad (2)$$

where  $W$  is the radiated power in watts and is determined by the formula:

$$W = \frac{1}{2} R_a u^2. \quad (3)$$

Here  $u$  is the vibrating velocity of the radiating surface and  $R_a$  is the radiation resistance. For a one-sided source, radiation resistance is

$$R_a = \pi \rho c S^2 / \lambda^2, \quad (4)$$

where  $\rho$  and  $c$  are the water density and the sound speed, respectively,  $S$  is the area of the radiating piston, and  $\lambda$  is the sound wavelength. Taking into account that  $u = F/Z$  (here  $F$  is the vibromotive force and  $Z$  is the load impedance for the vibromotive generator) and that in resonance  $Z = R_a + R_m$ , relationship (3) yields

$$W(a, f, R_m) = R_a F^2 / 2(R_a + R_m)^2. \quad (5)$$

Here  $a$  is the radius of the radiating piston and  $f$  is the frequency.

The efficiency of the electro-acoustical conversion  $\eta_{em}$  is the product of electro-mechanical efficiency  $\eta_{em}$  and mechano-acoustical efficiency  $\eta_{ma}$  (see Ref. 8):

$$\eta_{em} \approx \eta_{em} \times \eta_{ma}. \quad (6)$$

The efficiency of electro-mechanical conversion  $\eta_{em}$  for electric motors is very high (80%–90%). The efficiency of the mechano-acoustical conversion is

$$\eta_{ma}(a, f, R_m) = R_a / (R_m + R_a). \quad (7)$$

The  $Q$  factor is

$$Q(a, f, R_m) = 2\pi f (M_m + M_a) / (R_a + R_m), \quad (8)$$

where  $M_m$  is the mechanical mass of the radiator and  $M_a$  is the added mass of water. For a one-sided source

$$M_a = 2\rho a^3. \quad (9)$$

As can be seen from the above formulas, the mechanical resistance is one of the governing parameters for the radiator design. In conventional sound sources,  $R_m$  is determined by friction in deformed materials (radiating surface or its suspension, mechanical spring, etc.). The value of  $R_m$  for conventional sources is usually in the range 1000–5000 kg/s (mechanical ohms).

In our design using an air spring and the lack of material deformation,  $R_m$  can be much smaller and is determined mainly by friction in the gap between the floating body and the chamber. In this case we can estimate  $R_m$  according to the equation<sup>9</sup>

$$R_m \approx \frac{1}{2} \tilde{\rho} s \sqrt{\pi f \nu}, \quad (10)$$

where  $s$  is the area of the frictional contact between the float and the chamber, and  $\nu$  and  $\tilde{\rho}$  are the kinematic viscosity and the density of the liquid in the gap, respectively. From this formula,  $R_m$  is estimated to be in the range 10–100 kg/s, i.e., one or even two orders of magnitude less than that of conventional sources.

For the ocean thermometry projects suppose the source requirements to be  $f = 70$  Hz,  $SL = 200$  dB, bandwidth ( $SL = 197$  dB) = 12 Hz, efficiency > 70%. In order to evaluate the parameters for this source, let us consider the dependencies of the source level, mechano-acoustical efficiency, and the quality factor versus radius of the radiating surface (Fig. 5). The curves on this figure are plotted for frequency 70 Hz for four different values of the mechanical resistance  $R_m$ . Source level is normalized on 4.5 N (1 lb) force. The actual SL can be found by the formula

$$SL = SL^* + 20 \log F_{rms}, \quad (11)$$

where  $F_{rms}$  is the root mean square vibromotive force in pounds, and  $SL^*$  is the source level re: 1 lb force.

From these figures we examine two approaches for fulfilling the requirements for SL, efficiency, and bandwidth. Approach 1 is to get large radius and large force (example 1):

$$\text{radius } a = 1 \text{ m},$$

$$\text{force } F = 9300 \text{ N (2050 lb)},$$

$$SL = 200 \text{ dB re: } 1 \mu\text{Pa at } 1 \text{ m},$$

$$\text{bandwidth (SL = 197 dB) = 12 Hz},$$

$$\eta_{ma} > 0.9.$$

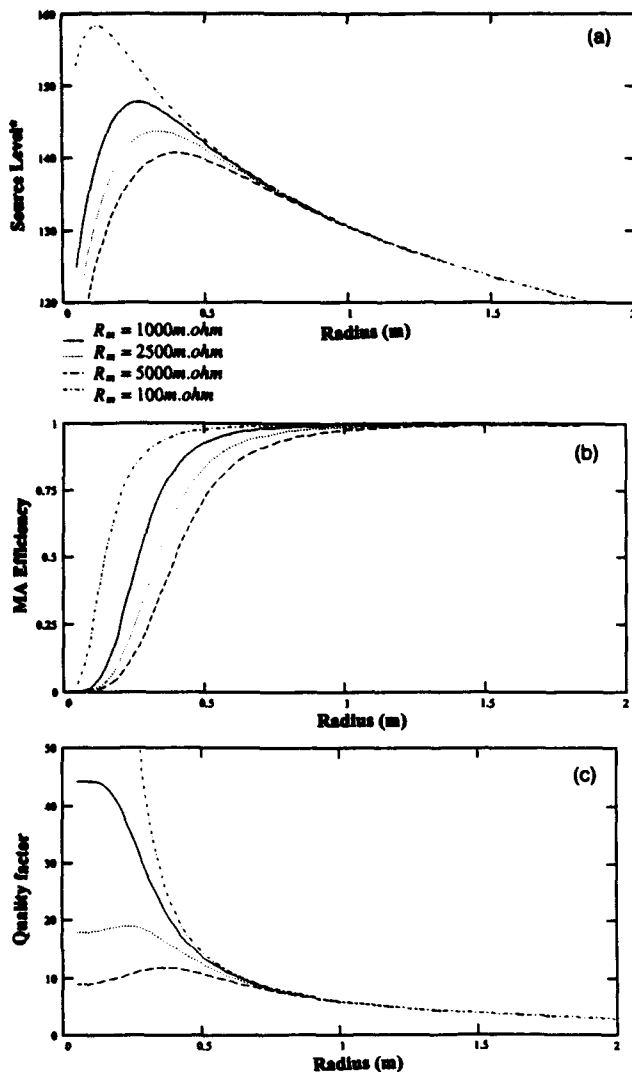


FIG. 5. The calculated characteristics of a sound source: (a) normalized source level, (b) mechano-acoustical efficiency, (c) quality factor as a function of the radius of the source for frequency 70 Hz. Each curve corresponds to different values of mechanical resistance.

The other approach uses smaller radiating surface. In this case the efficiency can still be high (in our design  $R_m$  is small); however, the bandwidth is narrower than desired. The bandwidth (with the required source level) can be extended by varying the force (example 2, Fig. 6):

$$\text{radius } a = 0.4 \text{ m,}$$

$$\text{force } F = 4500 \text{ N (1000 lb),}$$

$$\text{SL} = 207 \text{ dB re: } 1 \mu\text{Pa at } 1 \text{ m,}$$

$$\text{bandwidth (SL} = 197 \text{ dB)} = 12 \text{ Hz,}$$

$$\eta_{ma} > 0.9.$$

The cost of this approach is lower overall efficiency.

As can be seen, the second approach seems better than the first one. In the second example, higher source level, the same frequency band, and high-enough efficiency can be achieved with significantly smaller size and force. The

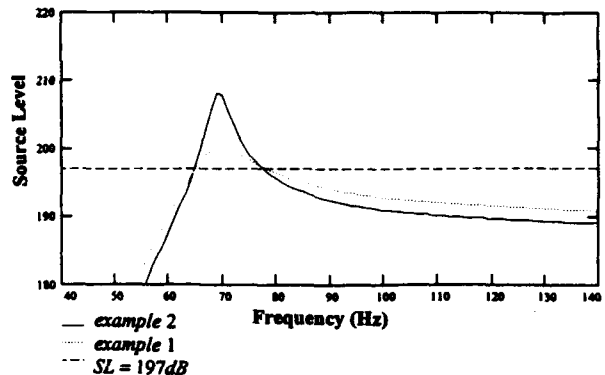


FIG. 6. Frequency responses of the source for example 1 (dashed curve) and example 2 (solid curve).

trade-off for this is the higher displacement of the radiating surface. (For the same source level, in example 2 the displacement is 6.25 times that of example 1.) Such a high displacement is quite acceptable for the proposed design (because of the lack of limitation for the displacement) and unacceptable for the conventional sound source design.

The conventional approach requires a large force generator and large size of the source, which leads to very high cost and low reliability and reduces the efficiency (larger size causes more friction).

### III. UTILIZATION OF GAS CAVITY AS SPRING

#### A. Radiator with variable resonance frequency

The use of a gas cavity as a spring and large relative displacement of the chamber and the float allows one to change the resonance frequency of the source by changing the stiffness of the gas spring. The stiffness  $k$  of the cylindrical gas volume in the chamber can be found from the adiabatic equation of state:

$$k = \gamma P_0 S / L, \quad (12)$$

where  $S$  is the area of the horizontal section of the cavity,  $L$  is its height,  $P_0$  is the equilibrium pressure of the gas (equal to hydrostatic pressure of water), and  $\gamma$  is the ratio of specific heats for the gas within the cavity. There are two ways to change  $k$ . One way is simply adding or releasing gas into or from the chamber. For the unchanged hydrostatic pressure, that will cause  $L$  to increase or decrease and, hence, will change the resonance frequency. The other way to control the resonance frequency is to change the depth of the submerged source because  $P_0$  and  $L$  are a function of the depth:

$$P_0 = P_{\text{atm}} (1 + 0.1H), \quad (13)$$

$$L(H) = L(H_0) (1 + 0.1H_0) / (1 + 0.1H),$$

where  $P_{\text{atm}} = 10^5 \text{ Pa}$  is the atmospheric pressure,  $H$  is the depth in meters, and  $H_0$  is an original (arbitrary) depth. For resonance frequency  $f_r$ , the relationships (1), (9), (12), and (13) yield

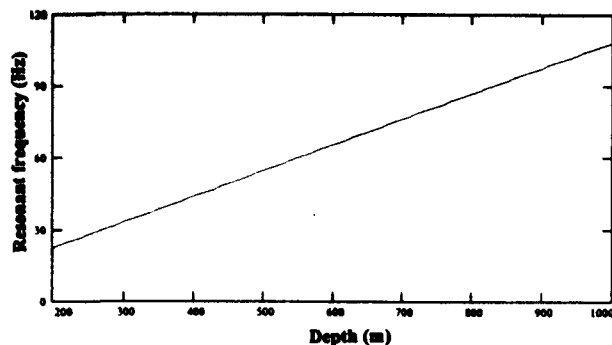


FIG. 7. Resonance frequency of the source versus depth.

$$f_r(H) = \frac{1}{2\pi} \sqrt{\frac{\gamma SP_{atm}}{L(H_0)(1+0.1H_0)(M_m+M_a)}} \times (1+0.1H). \quad (14)$$

Formula (14) shows linear dependence of resonance frequency with depth. An example of this for a radiator having radius  $a=0.4$  m,  $M_m=100$  kg, and  $L(H_0=300$  m)  $=0.22$  m is shown in Fig. 7.

### B. Multifrequency resonant radiator

An air spring with frequency-dependent stiffness can be used to create a multiresonant radiator. Figure 8(a) shows the similar scheme of the sound source as in Fig. 1(b) with an additional partition having a small opening. This partition divides the air chamber into two chambers having volumes  $V_0$  and  $V_1$  and forms a Helmholtz resonator with the volume  $V_1$  and the resonance frequency  $f_1$ . Figure 8(b) shows an equivalent electrical diagram of this source (for simplicity we consider the one sided mode of source operation). Here  $L_1$ ,  $C_1$ , and  $R_1$  are, respectively,

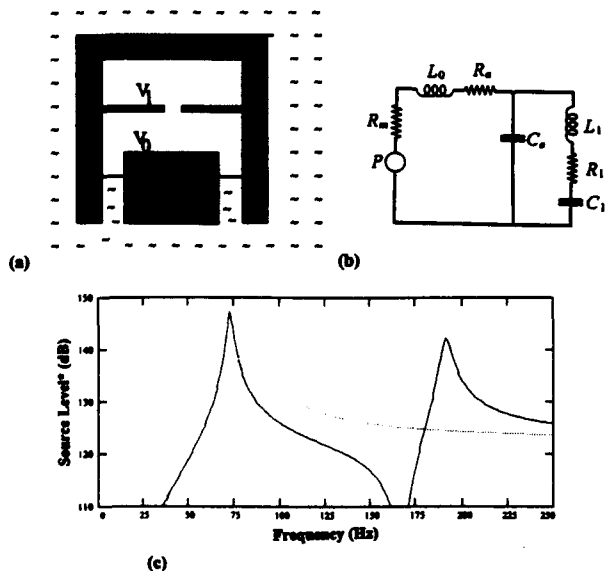


FIG. 8. Dual-frequency sound source: (a) two-chamber source, (b) equivalent electrical diagram, and (c) frequency response (dotted line is for the source without the partition).

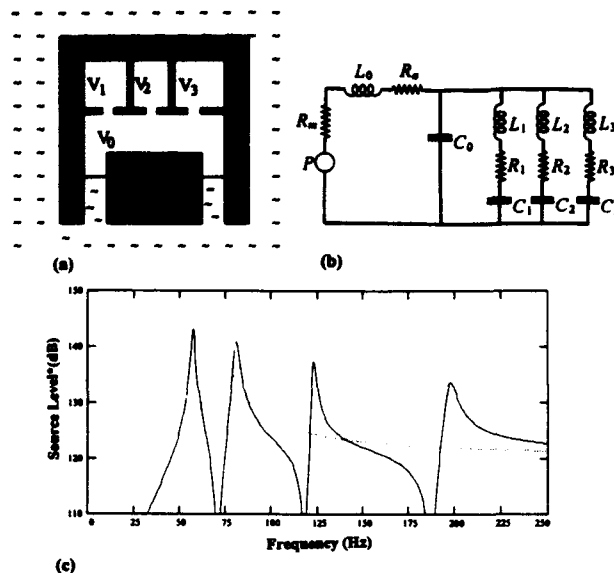


FIG. 9. Multifrequency source with four chambers: (a) diagram, (b) equivalent electrical diagram, (c) frequency response of the sources with four chambers (solid line). Dotted line is for the sources without the partitions.

inductance (inertia), capacitance (elasticity), and resistance (friction)<sup>10</sup> of the resonator,  $f_1 = 1/\sqrt{L_1 C_1}$ . Such a system may have two resonances and antiresonance between them. If the frequency  $f_1 > f_0$ , where  $f_0 = 1/\sqrt{L_0(C_0+C_1)}$  is the resonance of the source without the partition, this partition has little effect on the overall stiffness of the gas cavity with volume  $V_0+V_1$  and the first resonance of the source with partition is close to the frequency  $f_0$ . The frequency  $f_a$  of the antiresonance can be evaluated by

$$f_a \approx f_1 \sqrt{(V_1+V_0)/V_0}.$$

The second resonance frequency depends on all of the parameters  $C$ ,  $L$ , and  $R$  of the source and can be defined numerically. An example of the frequency response of the source with two air chambers is shown in Fig. 8(c). The graph in Fig. 8(c) is plotted for a one-sided source having the following parameters: radius of the radiating piston  $a=0.3$  m, mass of the float  $M=50$  kg, opening (in the partition) radius  $b=0.04$  m, both chambers have the same volume ( $V_0=V_1=0.02$  m<sup>3</sup>) on the depth  $H=1000$  m, mechanical resistance of the source  $R_m=1000$  mΩ. For this source  $f_0=83$  Hz,  $f_1=118$  Hz.

The sound source with  $n$  chambers will have  $n$  resonance frequencies, respectively. Figure 9 shows an example of the one-sided source with four chambers. The analysis of the frequency response of this source can be performed with equivalent electric diagram [Fig. 9(b)]. Frequency response (for 1 lb force) of the four-chambered source is shown in Fig. 9(c) for the following parameters: radius of the piston  $a=0.5$  m; radii of the openings  $b_1=0.012$  m,  $b_2=0.032$  m, and  $b_3=0.07$  m; volumes of the chambers on the depth 1000 m  $V_0=0.063$  m<sup>3</sup> and  $V_1=V_2=V_3=0.02$  m<sup>3</sup>; mass of the float  $m=100$  kg; and mechanical resistance  $R_m=1000$  mΩ.

This new feature of the source allows us to radiate sound efficiently and simultaneously in a few frequency bands or to switch radiation between different resonance frequencies and can be useful for various applications.

#### IV. CONCLUSION

The proposed underwater sound radiator has the following advantages: high reliability, because of the lack of material deformation, the use of highly reliable manufactured units (electric or linear motor) and very simple construction; high source level, in a low-frequency range due to less stringent limitations on the displacement of the radiating surface; high efficiency, due to the high efficiency of the electric (linear) motor and the low mechanical resistance of the proposed design; relatively low cost, due to the very simple construction and the use of mass-manufactured units (motors); and frequency diversity, due to properties of the air spring.

The proposed design of the radiator can be used for different applications (for NAVY, marine geology and oceanography, for deep as well as shallow water tomography) and can cover the frequency range from a few hertz up to hundreds of hertz because of the unique capability to generate a large displacement of a radiating surface without deformation of materials.

#### ACKNOWLEDGMENTS

The authors wish to thank Dr. M. Bruno for his support of this work, Mr. J. Nazalewicz for assistance in the design, and Mr. M. Reid and Mr. D. Meding for the construction of the experimental sound radiator.

- <sup>1</sup>R. C. Spindel and P. F. Worcester, "Ocean acoustic tomography: a decade of development," *Sea Technol.* 32, 47-52 (1991).
- <sup>2</sup>A. Baggeroer and W. Munk, "The Heard Island feasibility test," *Phys. Today* 45(9), 22-30 (1992).
- <sup>3</sup>J. L. Spiesberger and K. Metzger, "Basin-scale ocean monitoring with acoustic thermometers," *Oceanography* 5, 92-98 (1992).
- <sup>4</sup>F. Massa, "Sonar transducers," *Sea Technol.* 30(11), 39-48 (1989).
- <sup>5</sup>D. M. Donskoy, *Low Frequency Underwater Acoustic Radiator*. U.S. Patent No. 5,233,570 (1993).
- <sup>6</sup>J. E. Blue, A. L. Van Buren, and P. A. Semper, "A low-frequency, tow-powered sound source," in *Proceedings of the International Workshop "Power Transducers for Sonic and Ultrasonics"*, Toulon, France, 12-13 June 1990 (Springer-Verlag, Berlin, 1990), pp. 178-185.
- <sup>7</sup>R. J. Urick, *Principles of Underwater Sound* (McGraw-Hill, New York, 1983), 3rd ed., p. 75.
- <sup>8</sup>R. S. Woollett, *Sonar Transducer Fundamentals* (Naval Underwater System Center, New London, CT, 1992), p. 73.
- <sup>9</sup>G. K. Batchelor, *An Introduction to Fluid Dynamics* (Cambridge U.P., Cambridge, UK, 1967), pp. 353-364.
- <sup>10</sup>A. D. Pierce, *Acoustics* (Acoustical Society of America, Woodbury, NY, 1989), pp. 333-341.

Accession For	
NTIS CRA&I	<input checked="" type="checkbox"/>
DTIC TAB	<input type="checkbox"/>
Unannounced	<input type="checkbox"/>
Justification	
By	
Distribution /	
Availability Codes	
Dist	Avail and/or Special
A-1	20